Asian Journal of Pharmaceutical Sciences 15 (2020) 752–758

Available online at www.sciencedirect.com

ScienceDirect

journal homepage: www.elsevier.com/locate/AJPS

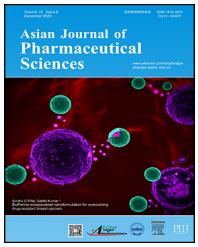

Original Research Paper

Oral uptake and persistence of the FnAb-8 protein characterized by in situ radio-labeling and PET/CT imaging

Qian Wang[a], Wangxi Hai[b], Sanyuan Shi[b], Jinliang Peng[b], Yuhong Xu[a,*]

[a] School of Pharmacy and Chemistry, DaLi University, Dali 671000, China
[b] School of Pharmacy, Shanghai Jiao Tong University, Shanghai 200240, China

ARTICLE INFO

Article history:
Received 19 May 2019
Revised 4 March 2020
Accepted 5 March 2020
Available online 21 March 2020

Keywords:
FcRn
IEDDA
Oral uptake

ABSTRACT

The absorption of peptides and proteins delivered orally is minimum because of the intestine epithelial barrier. There are few known active transport mechanisms for macromolecules including the neonatal Fc Receptor (FcRn) for the absorption and secretion of IgGs in infant and adult intestine. We had previously described the FnAb-8 protein that could bind to hFcRn tightly at pH 6.0 but barely at pH 7.4. In this study, we examined its uptake, biodistribution and pharmacokinetics after peroral administration in both wild-type and human FcRn transgenic (Tg) mice. FnAb-8 was modified to contain trans-cyclooctene (TCO) which could interact with ^{18}F labeled tetrazine in situ via the bioorthogonal inverse-electron-demand Diels–Alder reaction. We showed that FnAb-8 had a tendency to distribute and persist in the Tg mice intestine for an extended duration of time. It could also be absorbed into the circulation and distributed systemically over a long period of time up to 172 h. The improvement in oral uptake and concentration in the intestine tissue may be valuable for designing oral delivery of biopharmaceuticals, especially for diseases involving the gastric intestinal tissue.

1. Introduction

The neonatal Fc receptor (FcRn) was initially identified to be highly expressed on epithelial cells in the proximal small intestine in newborn rodents [1–3]. They are considered critical for the unidirectional transport of high fraction (~30%) of maternal IgG from suckled milk to the bloodstream [4]. But after weaning, the expression levels of FcRn decrease drastically in rodents, while in human and nonhuman primates, there are still considerable levels of FcRn found in the intestines and the proximal colon [5,6].

Based on these observations, oral absorption of macromolecular drugs via FcRn mediated transport mechanism was explored [7]. Muzammli et al. studied full-length mAbs given by endoscopic delivery to the intestine in primate models [8]. They observed detectable systemic exposure, but the plasma concentrations were below the

* Corresponding author. School of Pharmacy and Chemistry, DaLi University, No. 2, Hongsheng Road, Gucheng, Dali 671000, China. Tel.: +86 13501604118
E-mail address: yxhu@dali.edu.cn (Y.H. Xu).
Peer review under responsibility of Shenyang Pharmaceutical University.

https://doi.org/10.1016/j.ajps.2020.03.002

desirable therapeutic level. Claypool et al. modified the IgG Fc sequence to enable tighter binding to FcR at pH 6.0 and observed transcytosis through human intestinal cells [9]. Our lab reported a single-chain antibody fragment (scFv) FnAb-8 that could bind to hFcRn with higher affinity than IgG at pH 6.0 but similar or lower affinities than IgG at pH 7.4 [10]. Considering the slightly acidic gastric environment in maternal IgG transport in duodenum, we think FnAb-8 may also be able to bind to intestinal epithelial cells and be endocytosis. After endocytosis, they may again escape the fate of lysosome degradation and be recycled back to cell surfaces both ways.

But the characterization and quantification of the macromolecule delivery process have been difficult. Muzammli et al. used endoscopic delivery of enteric coated capsules in primates in order to control IgG release at the ileum but the measured plasma concentrations were still highly variable [8]. In this study we propose to record tomographic images during the macromolecule uptake and distribution phases, in order to characterize the extent and kinetics of the uptake in animal models. The FnAb-8 protein was labeled with the ^{18}F PET tracer and imaged using a microPET/CT device. Because FcRn expression in the intestine of rodents after weaning are very low and functionally irrelevant [11,12], we also examined FcRn Transgenic (Tg) mice and compared the images with those in wild type (WT) mice. Besides, because the fluorine-18 radionuclides has very short half-life and the protein uptake and distribution duration could be much longer, we adopted an *in situ* radionuclide labeling approach based on the reverse electron requirement Diels-Alder cycloaddition reaction [13].

The FnAb-8 protein was modified to contain the functional group trans-cyclooctene (TCO) and administered both by p.o. and i.v. in WT and Tg mice. At specific time points afterwards, ^{18}F labeled tetrazine (Tz-NOTA-Al^{18}F) was injected i.v. which would react with high efficiency and specificity with FnAb-8-TCO *in vivo*. We showed that FnAb-8 were detected systemically in Tg mice for up to a week after p.o. administration, and such labeling strategy enabled quantitative analysis of the pharmacokinetic and pharmacodynamic behavior of FnAb-8.

2. Materials and methods

2.1. Materials

The TCO-NHS ester, Tetrazine(Tz)-amine HCl salt, NOTA-NHS ester were purchased from Macrocyclics Inc. (Dallas, USA). ^{18}F fluorine was kindly supplied by Shanghai Atom Kexing Pharmaceuticals Co., Ltd. (Shanghai, China). All other chemicals, unless noted, were brought from Sinopharm Chemical Reagent Co., Ltd (Shanghai, China) and used without further purification. FnAb-8 scFv was expressed and purified as described [10].

2.2. Preparations of Tz-NOTA-AL^{18}F

The synthesis schemes were modified based on the published protocol [14]. Tz-NOTA was synthesized by first dissolving 14 mg of NOTA-NHS ester (2.5×10^{-2} mmol) in 600 µl of 0.1 M NaOH buffer, then adding the solution to 1 mg Tz-amine (2.5×10^{-3} mmol) in a 1.7 ml microcentrifuge tube, following by reaction for 1 h at RT with mild agitation. The resulted Tz-NOTA was obtained after reversed-phase C_{18} HPLC chromatography to remove unreacted NOTA-NHS ester. The collected product was frozen with liquid nitrogen and stored in the dark at −80 °C.

For the radio-labeling of Tz-NOTA, ^{18}F fluorine was obtained and the radio activities were quantified using a CRC-15R Dose Calibrator (Capintec). 10 µl of Tz-NOTA solution at 0.5 mg/ml (723 µM) and 50 µl of $AlCl_3$ solution at 2 mM were added into 400 µl of 0.2 M NH_4OAc pH 5.5 buffer followed by 2000 µCi of ^{18}F. After heating to 100 °C for 15 min, the reactant was purified using HPLC through a reversed-phase C_{18} column. The radioactive Tz-NOTA-Al^{18}F fraction was dried using a rotary evaporator and redissolved in 0.9% sterile saline for injection.

2.3. Preparation of FnAb-8-TCO conjugates

FnAb-8 was labeled with TCO in a 1.5 ml microcentrifuge tube. 2.4 mg/ml (0.1 µM) solution of FnAb-8 in 1 ml of phosphate buffered saline with pH adjusted to 8.8–9.0 was prepared and mixed with an appropriate volume of TCO-NHS in N,N-dimethylformamide (25 mg/ml) to reach the TCO: mAb reaction stoichiometry of 10:1. The mixture was kept at 4 °C with gentle shaking for 1 h. Afterwards, the modified antibody was obtained after ultracentrifugation using a 10,000-Dalton molecular weight cutoff filter units (Amicon Ultra 4; Millipore Corp.). These FnAb-8-TCOs may be store at 4 °C in the dark for more than 3 months.

2.4. Animal studies

The *in vivo* animal experiments were performed according to an approved protocol and under the ethical guidelines of the Shanghai Jiao Tong University Animal Care and Use Committee. WT mice were purchased from Shanghai Lingchang Biotechnology Co.,Ltd. The FcRn transgenic mice were purchased from Beijing Biocytogen Co., Ltd. All experimental animals are of SPF grade and housed in the experimental animal center of Shanghai Jiao Tong University under SPF conditions with a constant room temperature of 23 ± 1 °C and a light cycle of 12 h (lighting starts at 7:30 am).

FnAb-8-TCO-Tz-NOTA-Al^{18}F (short named FnAb-8-^{18}F) was also prepared *ex vivo* and administered by i.v. or p.o. to WT and Tg mice. PET/CT scans were done 4 h after the FnAb-8-^{18}F administration. Blood samples (100 µl) were obtained at 0.5, 1, 2, 3 and 4 h time points and quantified using a gamma radiation counter. The in situ labeling mice receive 200 µl of 0.01 µmol FnAb-8-TCO via tail vein or by oral gavage. At various time points (6, 12, 24, 48, 72, 96, 120, 144 or 168 h) afterwards, they were injected by i.v. 20 µCi of Tz-NOTA-Al^{18}F. PET/CT scans were done 4 h after the Tz-NOTA-Al^{18}F injection.

2.5. PET/CT imaging

PET/CT scans were done at 4 h after the injection of ^{18}F-tracers. The mouse was anesthetized with a 2%

isoflurane/oxygen gas mixture and scanned by an Inveon MM Platform (Siemens Preclinical Solutions, Knoxville, Tennessee, USA) with a computer-controlled bed and 85 mm transaxial and 57 mm axial fields of view (FOV). 10-min static PET scans were acquired. The images were reconstructed using the OSEM3D (Three-Dimensional Ordered Subsets Expectation Maximum) algorithm followed by MAP (Maximization/Maximum a Posteriori) or FastMAP provided by IAW. 3D regions of interest (ROIs) were drawn based on the anatomic structure and standardized uptake values (SUV) were determined. Images were processed using the Inveon Research Workplace (IRW) software v3.0.

3. Results and discussion

3.1. *The schemes for* in situ *labeling of FnAb-8 for PET imaging*

Positron emission tomography (PET) imaging has become an indispensable tool in the clinics for diagnosis and management of cancer. It is also highly useful in monitoring drug distribution and persistence in drug development [15,16]. Positron signals are especially sensitive and related noise or interferences are low. The signal intensities in the ROIs may directly correlate to the tracer concentration, allowing for quantitative analysis of drug distribution and their kinetic and dynamic changes in real time.

For labeling proteins and antibody “in situ” in aqueus or biological medium, the inverse electron-demand Diels-Alder followed by a retro [4 + 2] cycloaddition reaction may be prefered [13,19]. These reactions are “spring-loaded"—driven by a high thermodynamic force with high kinetics, high yield, and high reaction specificity [20]. Strained cyclooctenes can react with Tz with high efficiency. The electron-donating substituents on the dienophile and electron-withdrawing substituents on the diene accelerate the inverse-demand diels-alder. Such a IEDDA reaction between 1,2,4,5 Tz and TCO was reported and found to be well suited for in situ labeling of protein and antibody fragments [21,22].

The labeling reaction schemes were shown in Fig. 1. FnAb-8 was modified to contain TCO (Fig. 1B). Tz was conjugated to NOTA, followed by chelation of Al (III) and adsorption of ^{18}F (Fig. 1A). The reaction between FnAb-8-TCO with Tz-NOTA-Al^{18}F was confirmed *in vitro* when the reactants were mixed at 1:10 molar ratio and examined in HPLC using both radioactive and UV detectors as shown in Fig. 1D. The *ex vivo* labeled FnAb-8-^{18}F were used in animal studies in comparison with in situ labeled materials.

3.2. *The biodistribution of FnAb-8-^{18}F in WT and FcRn-Tg mice after i.v. injection*

Both WT and FcRn-Tg mice were injected by i.v. with the *ex vivo* radio-labeled protein FnAb-8-^{18}F while the control groups got only the probe Tz-NOTA-Al^{18}F. Each group contained at least 3 animals. PET/CT scans were done 4 h after the probe injection. Representative images were shown in Fig. 2A–2D. These images were dose and decay adjusted so the pixel intensities reflected the radioactive signal strength. We also determine the SUV-bw values of the different organs based on the PET/CT images and summarized the data in Fig. 2E and 2F.

Clearly, the probe Tz-NOTA-Al^{18}F was shown to be cleared quickly in both WT and Tg mice (Fig. 2A and 2C). The labeled FnAb-8-^{18}F persisted much longer and most prominently concentrated in the abdomen area, especially in the Tg mice (Fig. 2D). The total standardized uptake values (SUVs) in the intestine were calculated using the image analysis software and plotted in Fig. 2E and 2F. The SUV in both WT and Tg mice received only the Tz-NOTA-Al^{18}F were about 1, while the SUV in FcRn Tg mice received FnAb-8-^{18}F were about 2000, showing the longer persistence of FnAb-8 and its preferential distribution to the intestine. Such an effect should be mediated by FcRn, because in WT mice where the binding affinity by FnAb-8 was much weaker, the SUV numbers were only around 10. There were higher signals in the gallbladders and kidneys in WT mice, probably because the probes were metabolized and excreted faster in WT mice.

PET/CT signals have been used to quantify the absorption, PK and biodistribution of orally administered drugs in animals and in human [27,28]. But since PET imaging requires labeling of positron emitters and the most commonly available ^{18}F has a very fast decay, it is almost impossible to follow pre-labels agents with *in vivo* half-life longer than 6 h. These PET images were all taken at 4 h after the probe injection. For later time points, the use of in situ labeling strategy was essential.

3.3. *In situ labeling and PET/CT imaging after FnAb-8-TCO i.v. injection*

The entire time course of FnAb-8 distribution in FcRn Tg mice after i.v. injection was recorded using the in situ radio labeling approach. All the FcRn Tg mice received i.v. of the same doses of FnAb-8-TCO. At each specific time points (6, 12, 24 and 48 h) after the injection, a group of 3 mice were injected again by i.v. Tz-NOTA-Al^{18}F. They were scanned after another 4 h. So the PET/CT images in Fig. 3A and 3B were representative images from each time point group and they were taken at about 10, 16, 28 and 52 h after the FnAb-8-TCO injection. For comparison, we also examined WT mice with the same procedure. But the signals were hardly detectable. We showed only the image taken at the first time point (10 h after FnAb-8-TCO injection and 4 h after Tz-NOTA-Al^{18}F injection) in Fig. 3C. By analyzing all the images obtained at different time points, we summarized the SUV-bw values in the different organs and plotted in Fig. 3D. Again the radioactive signals were mostly in the intestines. The intestine value changes were re-plotted with time in Fig. 3E. to highlight the FnAb-8 signal persistence for longer than 52 h in Tg mice.

Most previous studies describing immuno-PET, *i.e.*, labeling of antibodies and antibody fragments for PET imaging, used longer live PET tracers including zirconium-89 (half-life: 78.4 h), and copper-64 (half-life: 12.7 h) [17]. But the longer probe persistence may lead to high signal background. Therefore a two-step labeling techniques were proposed that involved sequentially injections of antibodies and small molecule positron probes separately for them to interact *in situ*. The technique was also named as “pretargeting” because the antibodies were believed to bind to their targets first

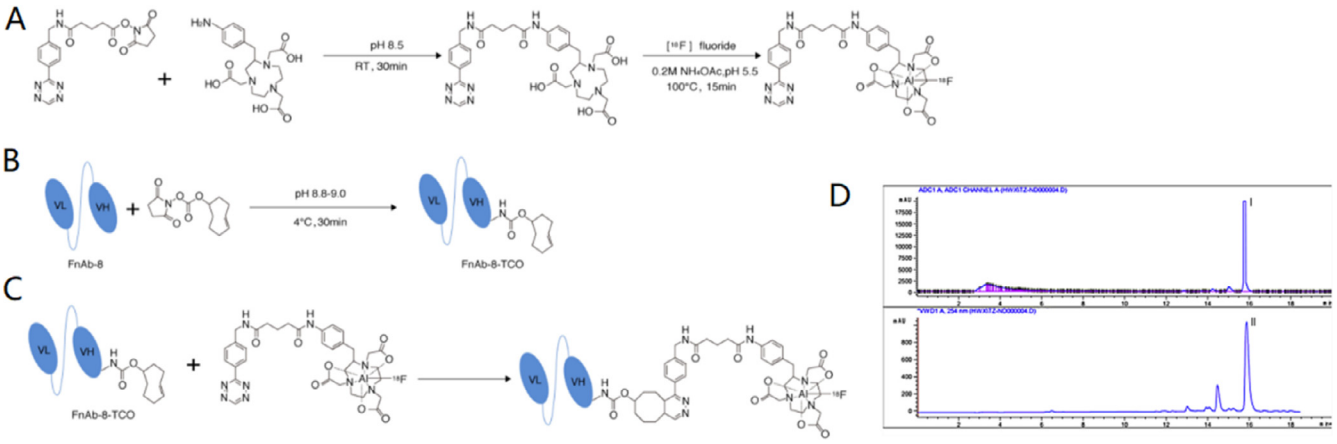

Fig. 1 – The reaction schemes of FnAb-8-TCO with Tz-NOTA-Al^{18}F. (A) The reaction for preparing Tz-NOTA-Al^{18}F. (B) The reaction for preparing FnAb-8-TCO. (C) The *in situ* labeling reaction. (D) HPLC chromatograms of Tz-NOTA-Al^{18}F with UV and radioactive detectors (I: radioactivity detection;II: UV signal detection 254 nm).

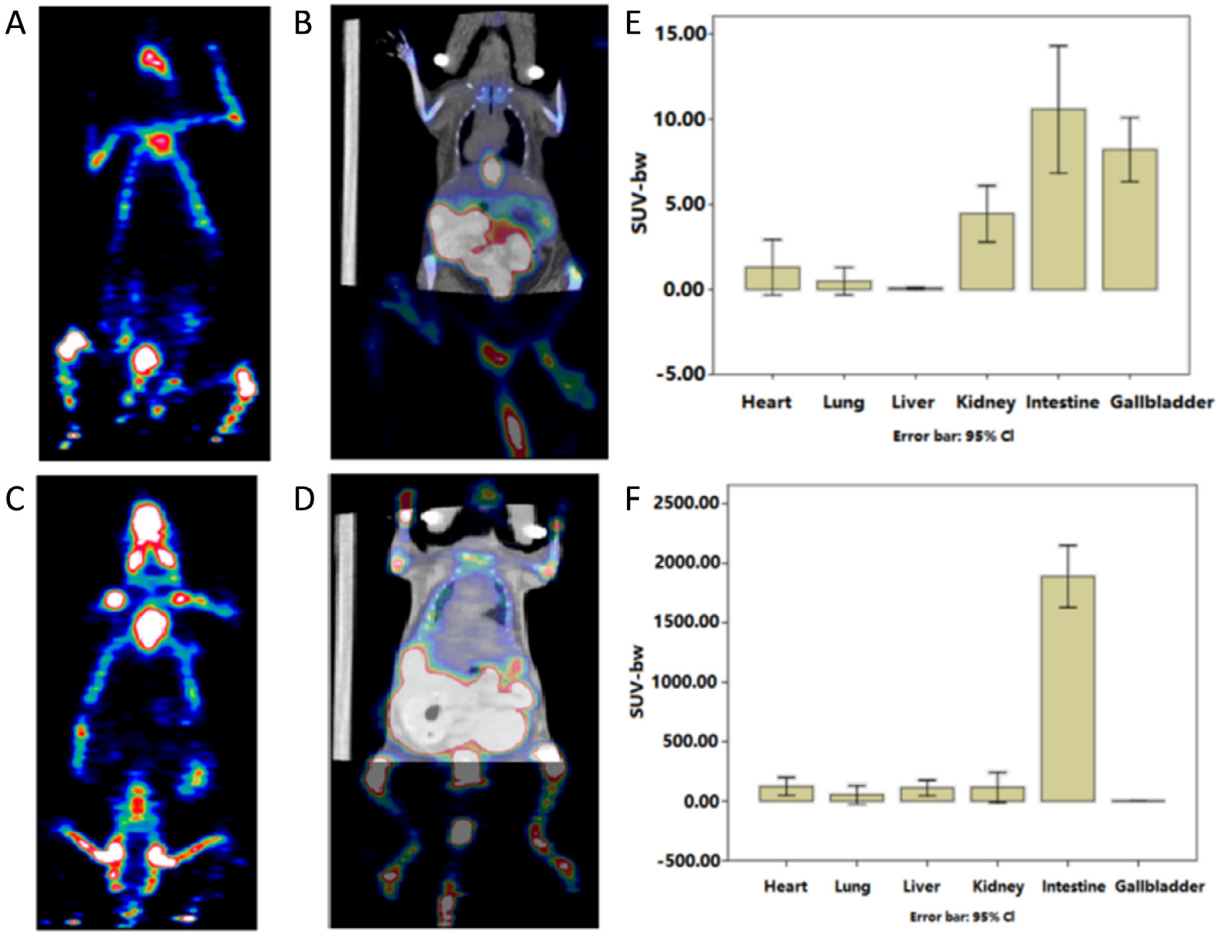

Fig. 2 – PET/CT images of WT and human FcRn Tg mice 4 h after i.v. of FnAb-8-^{18}F or Tz-NOTA-Al^{18}F. (A)WT mouse after i.v. of Tz-NOTA-Al^{18}F. (B) WT mouse after i.v. of FnAb-8-^{18}F. (C) Tg mouse after i.v. of Tz-NOTA-Al^{18}F. (D) Tg mouse after i.v. of FnAb-8-^{18}F. (E) SUV-bw values in different organs in WT mice after i.v. of FnAb-8-^{18}F. (F) SUV-bw values in different organs in human FcRn Tg mice after i.v. of FnAb-8-^{18}F.

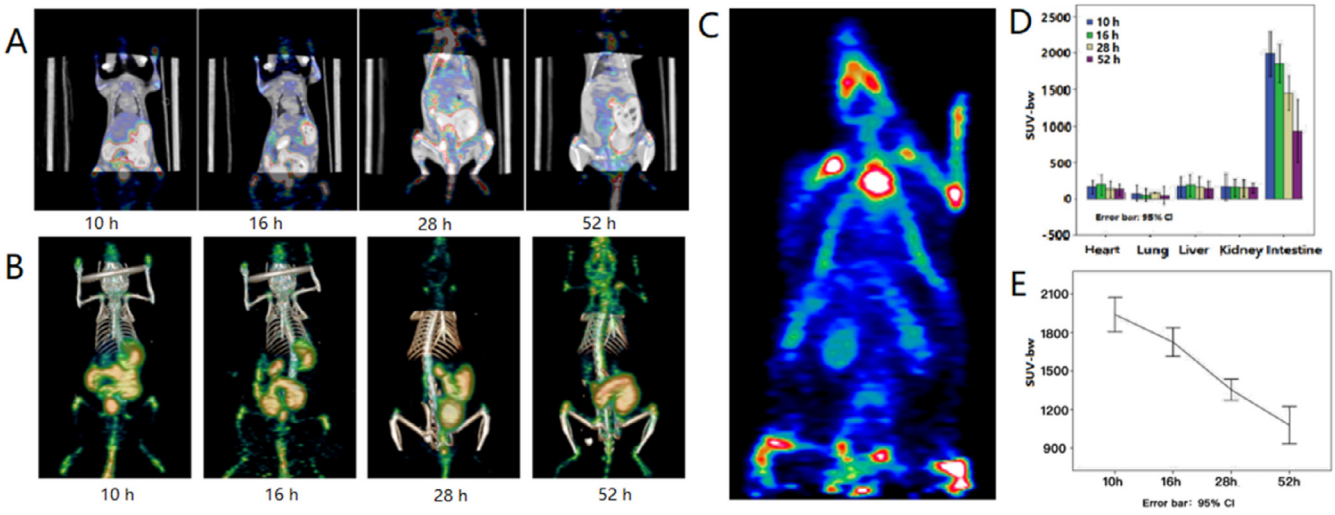

Fig. 3 – PET/CT imaging of FcRn Tg mice received i.v. of FnAb-8-TCO followed by in situ labeling by Tz-NOTA-Al^{18}F. (A) 2D images of Tg mice at 4 time points (from left to right). (B) 3D images of Tg mice at 4 time points (from left to right). (C) PET images of WT mice at 10 h after FnAb-8-TCO injection. (D) SUV values in various tissues in FcRn Tg mice. (E) SUV values in the intestines of FcRn Tg mice.

and then be labeled by the positron probe [18]. In our study, since FnAb-8 was not designed to targeted to FcRn on cell surfaces but for transporting by endosome FcRn, so the two step procedure was called in-situ labeling.

In this study, we were able to followed the entire time course of the protein distribution *in vivo*, based on the *in situ* labeling method. The signal accumulation in the intestine was noticed in FcRn mice. The drug concentration in the circulation was maintained for an extended duration, and signals in the intestine were seen after more than 52 h. We hypothesized that there may be continues two way transcytosis (recycling) of the FnAb-8 protein across the intestine epithelial cells in FcRn Tg mice.

3.4. *In situ labeling and PET/CT imaging after FnAb-8-TCO p.o. administration*

Similar situ labeling and PET/CT scans were done after p.o. administration of FnAb-8-TCO. At about 6, 12, 24, 48, 72, 96, 120, 144 and 168 h after the oral administration, a group of at least 3 mice were injected with Tz-NOTA-Al^{18}F and scanned in another 4 h. The representative PET/CT images at each time points were shown in Fig. 4A. The images were labeled with the PET/CT imaging time which were 10, 16, 28, 32, 76, 100, 124, 148 and 172 h after the p.o. administration. The FnAb-8 signals were found throughout the body but the intestine remained to be the most concentrated organ. The signals in other areas of the body suggested protein uptake and re-distribution via systemic circulation. They were detected at up to 172 h after the p.o. administration. In the control group, WT mice ($n = 4$) received the same experiment procedure but there was no signals detected even at the first time point (10 h after p.o. administration. The SUV-bw values in the intestines were calculated and plotted in Fig. 4B.

Almost all the previously reported two steps in situ labeling studies were done using intravenous injected drug and probes. In this study we were able to follow the time course of intestine absorption of FnAb-8 in FcRn mice based on *in situ* labeling using intravenously imaging probes. Since the probe Tz-NOTA-Al^{18}F was injected i.v. at various time points after the p.o. FnAb-8-TCO administration, they should most likely interact with the absorbed FnAb-8-TCO in circulation. Of cause it may be possible that the Tz-NOTA-Al^{18}F as a small molecule diffused out to the apical side of the intestine epithelial layer and reacted with FnAb-8-TCO. But the proportion should be limited. In order to confirm the in situ labeling occurred systemically, we further analyzed the blood samples drawn after FnAb-8-TCO p.o. administration Fig.4C.

3.5. *Gamma ray quantification in blood samples after i.v. and p.o. administration*

FnAb-8-^{18}F was administered either by i.v. or p.o. to FcRn Tg mice. Blood samples were drawn at 0.5 h, 1 h, 2 h, 3 h, 4 h after administration. The radioactivities were quantified using a gamma radiation counter and plotted in Fig. 5B and 5C. In addition, control group mice were injected with Tz-NOTA-Al^{18}F and their blood samples were also measured (Fig. 5A). The values in both i.v. and p.o. injected groups were higher and persisted longer. Substantial oral absorption was observed with T_{max} at 1 h after p.o administration (Fig. 5C). Since the FnAb-8-NOTA clearance from the plasma should be similar regardless the administration routes, the Pk clearance profile in Fig. 5B and 5C were similar.

When comparing the radio-signals after p.o. *vs.* i.v. administration of FnAb-8-TCO, the bioavailability could be estimated to be quite significant. The results were remarkable considering we showed the entire time course of FnAb-8 absoption. Polypeptides and proteins are considered too big to be absorbed orally. But we hypothesized that the FnAb-8

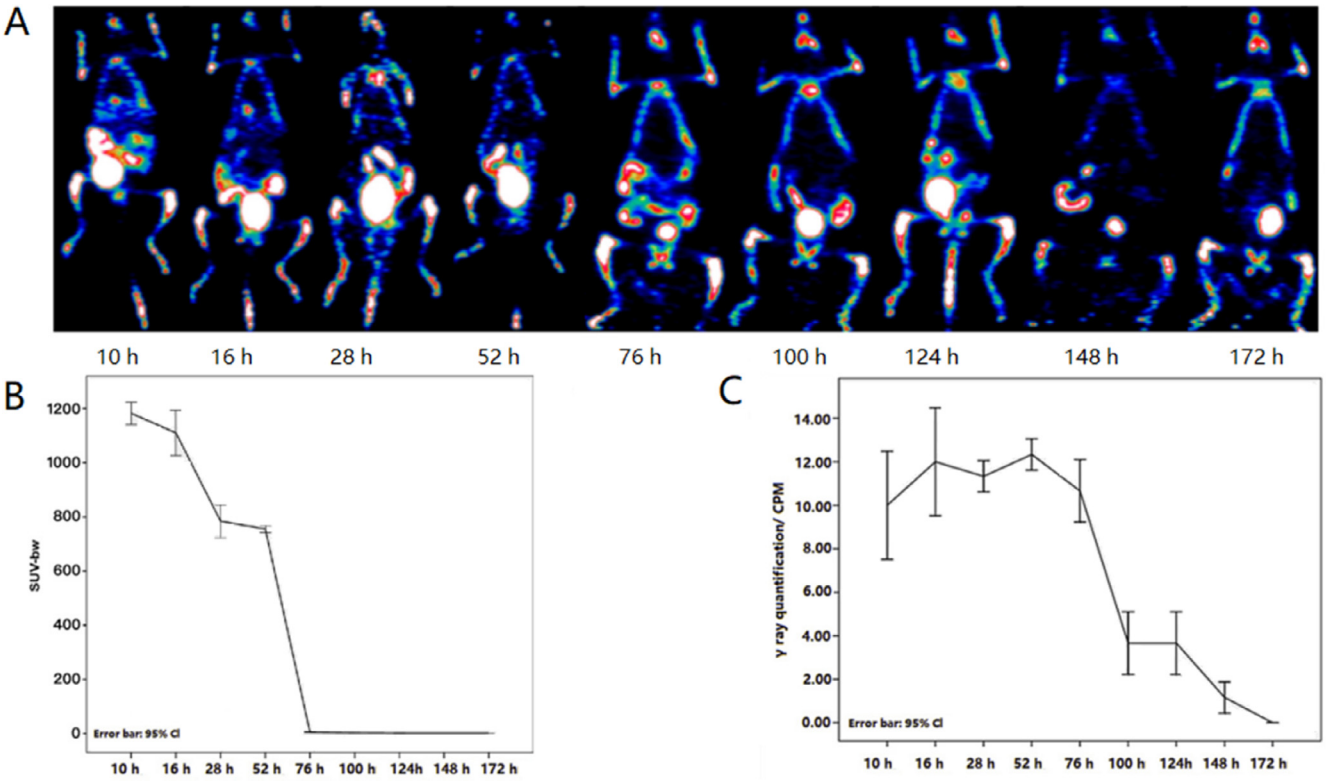

Fig. 4 – PET/CT imaging of FcRn Tg mice received p.o. administration of FnAb-8-TCO followed by in situ labeling by Tz-NOTA-Al^{18}F. (A) PET/CT Images of Tg mice at different times after oral administration of FnAb-8-TCO followed by *in situ* labeling by Tz-NOTA-Al^{18}F. (B) SUV-bw measurements in the intestine at different time points. (C) γ ray quantification of blood samples from Tg mice after oral FnAb-8-TCO followed by i.v. Tz-NOTA-Al^{18}F.

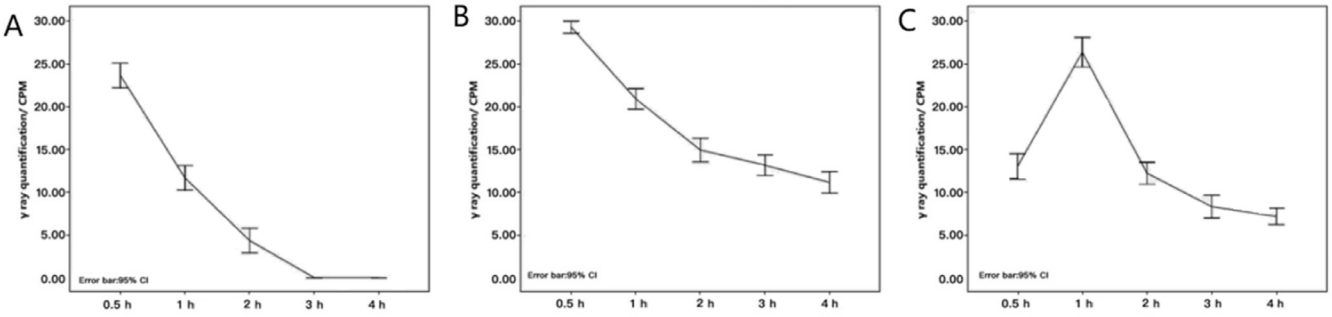

Fig. 5 – *γ ray quantification of blood sample of various samples*. (A) γ ray quantification of blood sample from Tg mice received iv Tz-NOTA-Al^{18}F. (B) γ ray quantification of blood sample from Tg mice received i.v. FnAb-8–^{18}F. (C) γ ray quantification of blood sample from Tg mice received p.o. FnAb-8–^{18}F.

protein may behave differently because of its affnity toward human FcRn [23–25]. FcRn mediated IgG transcytosis had been speculated by Haymann et al. who showed the presence of FcRn on glomerular epithelial cells as well as in the brush border of proximal tubular cells in the kidney [26]. Muzammil et al. engineered an IgG2 mAb for optimal FcRn binding, and it was formulated, lyophilized, and loaded into enteric-coated capsules for oral dosing in cynomolgus [8]. Absorption was observed in the small intestine in cynomolgus where pH was about 7.5 using the IntelliCap System. But they concluded that FcRn mediated IgG transport was not sufficient for mAbs to reach systemic therapeutic concentration. Our finding indicated that in addition to the possibility of oral uptake, the most significant feature of FnAb-8 and its conjugates is that they can maintain high concentration in the intestine for a long time. There may be highly valuable applications in this regard for drug delivery for diseases involving the intestine or colon.

4. Conclusion

In this study, we developed an in situ labeling mechanism based on a retro [4+2] cycloaddition reaction, in order

to follow the biodistribution of FnAb-8 after i.v. and p.o. administration using PET imaging. FnAb-8 was found to persist longer in FcRn transgenic mice and accumulated in the intestine tissues for an extended duration. These observations suggested FnAb-8 may have an unique property to be absorbed orally and be used as an carrier for delivery to the intestine tissues.

Conflicts of interest

The authors declare that there is no conflicts of interest.

Acknowledgments

The authors would like to thank Ruijin Hospital PET center for supports in carrying out the imaging studies using microPET. This project is funded by the Natural Science Foundation of China (Grant no. 81690262).

REFERENCES

[1] Hornby PJ, Cooper PR, Kliwinski C, Ragwan E, Mabus JR, Harman B, et al. Human and non-human primate intestinal FcRn expression and immunoglobulin G transcytosis. Pharm Res 2014;31(4):908–22.
[2] Antohe F, Rădulescu L, Gafencu A, Ghe V, Simionescu M. Expression of functionally active FcRn and the differentiated bidirectional transport of IgG in human placental endothelial cells. Hum Immunol 2001;62:93–105.
[3] Shah U, Dickinson BL, Blumberg RS, Simister NE, Lencer WI, Walker WA. Distribution of the IgG Fc receptor, FcRn, in the human fetal intestine. Pediatr Res 2003;53(2):295–301.
[4] Martin WL, West APJ, Gan L, Bjorkman PJ. Crystal structure an 2.8 A of an FcRn/heterodimeric Fc complex: mechanism of pH depedent binding. Mol Cell 2001;7(4):867–77.
[5] Israel EJ, Taylor S, Wu Z, Mizoguchi E, Blumberg RS, Bhan A, et al. Expression of the neonatal Fc receptor, FcRn, on human intestinal epithelial cells. Immunology 1997;92(1):69–74.
[6] Hornby PJ, Cooper PR, Kliwinski C, Ragwan E, Mabus JR, Harman B, et al. Human and non-human primate intestinal FcRn expression and immunoglobulin G transcytosis. Pharm Res 2014;31(4):908–22.
[7] Shen WC. Oral peptide and protein delivery: unfulfilled promises? Drug Discov Today 2003;8(14):607–8.
[8] Muzammil S, Mabus JR, Cooper PR, Brezski RJ, Bement CB, Perkinson R, et al. FcRn binding is not sufficient for achieving systemic therapeutic levels of immunoglobulin G after oral delivery of enteric-coated capsules in cynomolgus macaques. Pharmacol Res Perspect 2016;4(3):e00218.
[9] Claypool SM, Dickinson BL, Wagner JS, Johansen FE, Venu N, Borawski JA, et al. Bidirectional transepithelial IgG transport by a strongly polarized basolateral membrane Fcgamma-receptor. Mol Biol Cell 2004;15(4):1746–59.
[10] Qiu Y, Lv W, Xu M, Xu Y. Single chain antibody fragments with pH depedent binding to FcRn enabled prolonged circulation of therapeutic peptide *in vivo*. J Control Release 2016;229:37–47.
[11] Benlounes N, Chedid R, Thuillier F, Desjeux JF, Rousselet F, Heyman M. Intestinal transport and processing of immunoglobulin G in the neonatal and adult rat. Biol Neonate 1995;67(4):254–63.
[12] Kliwinski C, Cooper PR, Perkinson R, Mabus TR, Tam SH, Wilkinson TM, et al. Contribution of FcRn binding to intestinal uptake of IgG in suckling rat pups and human FcRn-transgenic mice. Am J Physiol Gastrointest Liver Physiol 2013;304(3):G262–70.
[13] Rossin R, Läppchen T, van den Bosch SM, Laforest R, Robillard MS. Diels-Alder reaction for tumor pretargeting: *in vivo* chemistry can boost tumor radiation dose compared with directly labeled antibody. J Nucl Med 2013;54(11):1989–95.
[14] Reiner T, Lewis JS, Zeglis BM. Harnessing the bioorthogonal inverse electron demand Diels-Alder cycloaddition for pretargeted PET imaging. J Vis Exp 2015;96:e52335.
[15] Willmann JK1, van Bruggen N, Dinkelborg LM, Gambhir SS. Molecular imaging in drug development. Nat Rev Drug Discov 2008;7(7):591–607.
[16] Tucker WE, Guglieri-Lopez E, Ordonez AA, Ritchie B, Klunk MH, Sharma R, et al. Noninvasive ^{11}C-ifampin positron emission tomography reveals drug biodistribution in tuberculous meningitis. Sci Transl Med 2018;10(470):eaau0965.
[17] Carmon KS, Azhdrinia A. Application of immuno-PET in antibody-drug conjugate develoment. Mol Imaging 2018;17(1):1536012118801223.
[18] Bailly C, Bodet-Milin C, Rousseau C, Faivre-Chauvet A, Kraeber-Bodéré F, Barbet J. Pretargeting for imaging and therapy in oncological nuclear medicine. EJNMMI Radiopharm Chem 2017;2:6.
[19] Meyer JP, Houghton JL, Kozlowski P, Abdel-Atti D, Reiner T, Pillarsetty NV, et al. ^{18}F-based pretargeted PET imaging based on bioorthogonal Diels-Alder click chemistry. Bioconjug Chem 2016;27(2):298–301.
[20] Fujiki K, Yano S, Ito T, Kumagai Y, Murakami Y, Kamigaito O, et al. A one-pot three-component double-click method for synthesis of [^{67}Cu]-labeled biomolecular radiotherapeutics. Sci Rep 2017;7(1):1912.
[21] Rossin R, Lappchen T, Bosch SM, Laforest R, Robillard MS. Diels-Alder reaction for tumor pretargeting: *in vivo* chenistry can boost tumor radiation dose compared with directly labeled antibody. J Nucl Med 2013;54(11):1989–95.
[22] Rossin R, van den Bosch SM, Ten Hoeve W, Carvelli M, Versteegen RM, Lub J, et al. Highly reactive trans-cyclooctene tags with improved stability for Diels-Alder chemistry in living systems. Bioconjug Chem 2013;24(7):1210–17.
[23] Israel EJ, Taylor S, Wu Z, Mizoguchi E, Blumberg RS, Bhan A, et al. Expression of the neonatal Fc receptor, FcRn, on human intestinal epithelial cells. Immunology 1997;92(1):69–74.
[24] Spiekermann GM, Finn PW, Ward ES, Dumont J, Dickinson BL, Blumberg RS, et al. Receptor-mediated immunoglobulin G transport across mucosal barriers in adult life: functional expression of FcRn in the mammalian lung. J Exp Med 2002;196(3):303–10.
[25] Heidl S, Ellinger I, Niederberger V, Waltl EE, Fuchs R. Localization of the human neonatal Fc receptor (FcRn) in human nasal epithelium. Protoplasma 2016;253(6):1557–64.
[26] Haymann JP, Levraud JP, Bouet S, Kappes V, Hagege J, Nguyen G, et al. Characterization and localization of the neonatal Fc receptor in adult human kidney. J Am Soc Nephrol 2000;11(4):632–9.
[27] Shingaki T, Takashima T, Wada Y, Tanaka M, Kataoka M, Ishii A, et al. Imaging of gastrointestinal absorption and biodistribution of an orally administered probe using positron emission tomography in humans. Clin Pharmacol Ther 2012;91(4):653–9.
[28] Yamashita S, Takashima T, Kataoka M, Oh H, Sakuma S, Takahashi M, et al. PET imaging of the gastrointestinal absorption of orally adminidtered drugs in conscious and anesthetized rats. J Nucl Med 2011;52(2):249–56.